#Liu Yu¹⁾, Yu Peng¹⁾, Zhang Luolei¹⁾, Zhao Chongjin¹⁾, Huang Zuwei¹⁾ (1 同済大学

Magnetotelluric Probability Tomography Based on the Correlation between **Impedance Perturbations and the Fréchet Operators**

#Yu Liu¹⁾, Peng Yu¹⁾, Luolei Zhang¹⁾, Chongjin Zhao¹⁾, Zuwei Huang¹⁾ (1 Tongji University

Probability Tomography, which was initially proposed by Patella (1997), has been extensively applied across geophysical exploration fields. The method calculates a probability value for each subsurface node, which quantifies the likelihood of an anomalous source (e.g., a charge, dipole, or physical property contrast) existing at that location.

The magnetotelluric (MT) probability tomography (Mauriello, 1999) uses electromagnetic induction field components (Equations 1 and 2) to derive charge-occurrence probability for TM mode (Equation 3) and dipole-occurrence probability for TE mode (Equation 4), thereby enabling a rapid reconstruction of the probable geometry of anomalous bodies without costly iteration. Here, the terms $(x-x_n)/[(x-x_n)^2+z_n^2]$ and $-z_m/[(x-x_m)^2+z_m^2]$ represent the space domain electric and magnetic tomography scanners, respectively.

However, this MT probability tomography employs frequency-independent scanners, neglecting the differential contributions of subsurface structures to the surface frequency response. To overcome this drawback, we introduce a novel probability tomography approach founded on the correlation of impedance perturbations with the Fréchet operators, as derived from the first-order Taylor expansion of the MT impedance (Equation 5). Its core principle involves calculating the correlation between the field generated by a unit source at the subsurface node and the measured anomalous field. This advancement allows effective integration of multi-frequency data.

To implement this method, the subsurface region is discretized into Q elementary cells, each with constant resistivity. The background impedances are obtained through forward modeling of a reference model, while the Fréchet operators are computed using the adjoint-state method. Thus, the core probability function for this technique is defined by Equation 6, where L is the number of frequencies, N is the number of measuring points, and W_d is the data weight matrix, which balances the disparities across different frequencies and measurement errors.

The effectiveness of the proposed method has been validated through extensive synthetic model tests (Figure 1 is result of synthetic three-block model). The results demonstrate that our method can characterize the morphology, boundaries, and depth extent of anomalous bodies with remarkable computational efficiency. This approach effectively mitigates the inherent limitations of conventional probability tomography, particularly its insufficient ability to differentiate between the depth and the resistivity values of anomalous bodies. Integrating the probability distributions of the TE and TM modes with the reference model's allows for the construction of an initial model that more closely approximates the true geological structure. This provides reliable initial constraints for subsequent inversion, significantly enhancing its convergence speed and the reliability of the final model. In addition, we applied the method to a real dataset acquired from the Junggar Basin.

$$\mathbf{E}(\mathbf{r}) = \frac{1}{4\pi\varepsilon_0} \sum_{n=1}^{N} \frac{\Gamma_n(\mathbf{r} - \mathbf{r}_n)}{|\mathbf{r} - \mathbf{r}_n|^3} + \frac{\mu_0 \omega^2}{4\pi} \sum_{m=1}^{M} \frac{\mathbf{P}_m}{|\mathbf{r} - \mathbf{r}_m|}$$
(1)

$$\mathbf{H}(\mathbf{r}) = \frac{i\omega}{4\pi} \sum_{m=1}^{M} \nabla \times \frac{\mathbf{P}_{m}}{|\mathbf{r} - \mathbf{r}_{m}|}$$
 (2)

$$\eta_{x}^{E}(x_{n}, z_{n}) = \frac{\sqrt{z_{n}} \int_{-\infty}^{+\infty} E_{x}(x) \frac{x - x_{n}}{(x - x_{n})^{2} + z_{n}^{2}}}{\sqrt{\frac{\pi}{2}} \int_{-\infty}^{+\infty} E_{x}^{2}(x) dx}$$
(3)

$$\eta_x^H(x_m, z_m) = \frac{\sqrt{z_m} \int_{-\infty}^{+\infty} H_x(x) \frac{-z_m}{(x - x_m)^2 + z_m^2}}{\sqrt{\frac{\pi}{2}} \int_{-\infty}^{+\infty} H_x^2(x) dx}$$
(4)

$$\Delta \mathbf{Z}(l,n) = \mathbf{Z}(l,n) - \mathbf{Z}^{ref}(l,n) = \sum_{i=1}^{Q} \frac{\partial \mathbf{Z}^{ref}(l,n)}{\partial \rho_{i}} \Delta \rho_{q}$$
(5)

$$\eta_{x}^{H}\left(x_{m}, z_{m}\right) = \frac{\sqrt{z_{m}} \int_{-\infty}^{\infty} H_{x}\left(x\right) \frac{-z_{m}}{\left(x - x_{m}\right)^{2} + z_{m}^{2}}}{\sqrt{\frac{\pi}{2}} \int_{-\infty}^{+\infty} H_{x}^{2}\left(x\right) dx} \qquad (4)$$

$$\Delta \mathbf{Z}(l, n) = \mathbf{Z}(l, n) - \mathbf{Z}^{ref}\left(l, n\right) = \sum_{q=1}^{p} \frac{\partial \mathbf{Z}^{ref}\left(l, n\right)}{\partial \rho_{q}} \Delta \rho_{q} \qquad (5)$$

$$\eta_{q} = \frac{\sum_{l=1}^{L} \sum_{n=1}^{N} W_{d}\left(l, n\right) \Delta \mathbf{Z}(l, n) \frac{\partial \mathbf{Z}^{ref}\left(l, n\right)}{\partial \rho_{q}}}{\sqrt{\sum_{l=1}^{L} \sum_{n=1}^{N} \left[W_{d}\left(l, n\right) \Delta \mathbf{Z}(l, n)\right]^{2} \cdot \sum_{l=1}^{L} \sum_{n=1}^{N} \left[\frac{\partial \mathbf{Z}^{ref}\left(l, n\right)}{\partial \rho_{q}}\right]^{2}} \qquad (6)$$

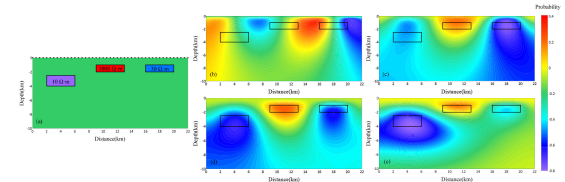


Figure 1. Comparison of imaging methods for the synthetic three-block model. (a) True model. (b) nventional TM-mode result (charge probability at 10Hz). (c) Conventional TE-mode result (dipole probability at 10Hz). (d) Proposed probability tomography (TM model). (e) Proposed probability tomography (TE model).